A Model Study of CO−CO Adsorbate Interaction on Si(100)-2×1

F. Bacalzo-Gladden and M. C. Lin*

Department of Chemistry, Emory University, Atlanta, Georgia 30322

Received: May 14, 1999

The CO−CO adsorbate interaction on Si(100)-2×1 has been investigated with ab initio molecular orbital and hybrid density functional theory calculations using cluster models of the surface. Different adsorption combinations for one and two CO molecules on single- and double-dimer cluster models, Si_9H_{12} and $Si_{15}H_{16}$, respectively, are described. Our calculations indicate that the second CO molecule is physisorbed on the same surface Si dimer where the first CO molecule is chemisorbed. The chemisorption of the first CO molecule induces a change in the charge of the surface Si dimer atoms which inhibits further adsorbate−surface interaction. The dissociation energy of the physisorbed second CO molecule is less than 1 kcal/mol. Adsorption of the second CO molecule on the second Si dimer is energetically preferred over coadsorption of CO on the same Si dimer. The 2OC-normal.d14 structure is the most stable configuration, with the two CO molecules adsorbed diagonally across the two Si dimers. The dissociation energy of the chemisorbed second CO molecule in the 2OC-normal.d14 structure is 13.8 kcal/mol, about 4 kcal/mol less stable than the first adsorbed CO. Adsorption of two CO molecules in a bridge configuration indicates a weak surface−adsorbate and/or adsorbate−adsorbate interaction. The dissociation energy of the single chemisorbed CO in the bridged state is 5.0 kcal/mol while that of the second CO is 1.7 kcal/mol. A mixed configuration, i.e., OC-normal with OC-bridge, was found to be unstable based on the $Si_{15}H_{16}$ surface model.

Introduction

There have been several studies conducted to investigate the interaction of CO with Si single-crystal surfaces[1−10] including the measurement for the vibrational spectrum of the adsorbed CO on Si(100)-2×1, first reported by Bu et al.[9] The results of these studies indicate that while CO adsorbs weakly on the reconstructed Si(100)-2×1 surface, it does not adsorb on the reconstructed Si(111)-7×7 surface even under very high-exposure conditions.[5,9]

The adsorption of CO on the Si(100)-2×1 surface has been investigated recently using first principles quantum chemical methods,[11] molecular dynamics calculations,[12] and ab initio molecular orbital and density functional methods.[13] Hu et al.[11] observed a nonthermally accessible phase for CO on the Si-(100) surface using an energetic molecular beam of CO. They characterized this new phase using density functional theory and Hartree−Fock calculations with the Si_9H_{12} cluster model. They found that thermal CO leads to the T-CO phase (one CO terminal bound to one Si of each dimer) and translationally energetic CO leads to a new BT-CO phase which is a combination of T-CO and bridge bound B-CO phase (one CO symmetrically bound to both atoms of the dimer). Imamura et al.[12] performed first-principles molecular dynamics calculations with a repeated slab model for the CO/Si(100) system and found two adsorption sites of CO on the Si(100) surface. One is where the CO adsorbed symmetrically and the other asymmetrically. In their calculations, they found that the asymmetric structure is energetically preferable although the calculated adsorption energy is 19.0 kcal/mol for the asymmetric one and 17.0 for the symmetric one. Both values are larger than the experimental activation energy (10.71−12.68 kcal/mol) for desorption.[11,14]

Recently, we have independently carried out ab initio molecular orbital (MO) and density functional theory calculations to investigate the adsorption of CO on the Si(100)-2×1 surface using the Si_9H_{12} and $Si_{13}H_{20}$ cluster models of the surface.[13] Our results were found to be in good agreement with experiment and with those obtained by Hu et al.[11] in which (i) the OC-normal (or T-CO phase) structure is more stable than the OC-bridge (or B-CO phase) and (ii) the formation of the OC-normal adsorbate occur without a reaction barrier. Furthermore, we reported that the B3LYP/6-31G(d) is a reasonable level of theory for the calculation of the geometries of the clusters and adsorbates, as well as the energetics of the CO/Si(100)-2×1 surface, and that the Si_9H_{12} cluster is a good model for the single-dimer system. The latter point has also been demonstrated by the groups of Carter,[15] Hoffmann,[16] and Doren.[17]

Despite all these studies, the nature of adsorbate interaction on the Si surface and the mechanisms involved have not been investigated. Therefore, in this work, we continue our previous studies of molecular adsorption and reactions on a model Si-(100)-2×1 surface. Our goal is to elucidate the interaction of CO with the CO/Si(100)-2×1 surface which has one CO either on a single-dimer cluster or on an adjacent double-dimer cluster model, using ab initio molecular orbital and density functional theory methods. Our emphasis is to examine the CO−CO adsorbate interaction and the effect of this interaction on the adsorption mechanism on the silicon surface. The results are systematically presented herein.

Computational Procedure

We have used two different surface models in this paper to represent the reconstructed Si(100)-2×1 surface. The first model is a Si_9H_{12} cluster, where the top layer is a dimer consisting of two Si atoms, each with one dangling bond.[11,13,15−16] This cluster will be referred to as the single-dimer model. The second model

* chemmcl@emory.edu.

10.1021/jp991590u CCC: $18.00
Published on Web 08/10/1999

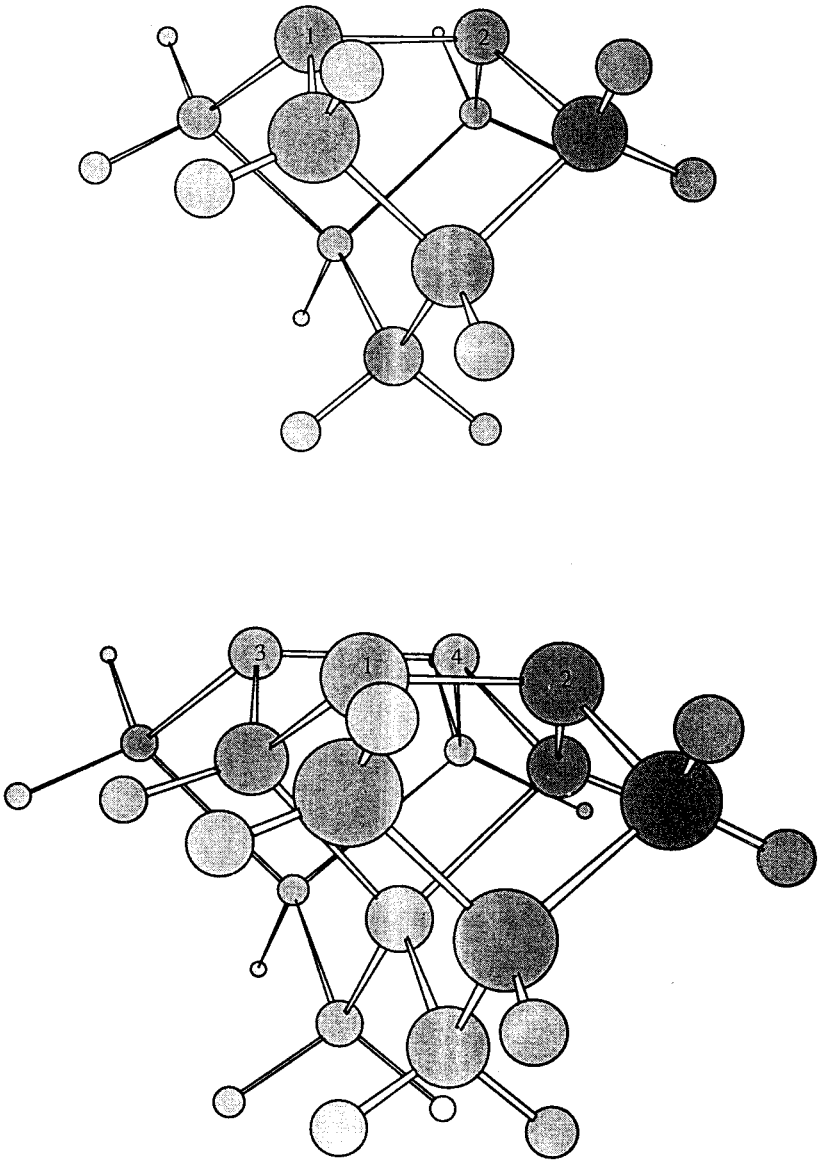

Figure 1. Optimized geometries of the Si_9H_{12} single- and the $Si_{15}H_{16}$ double-dimer models with the surface Si atoms labeled accordingly.

is a $Si_{15}H_{16}$ cluster, where the top layer consists of two adjacent dimers in the same dimer row.[17] The double-dimer model allows the study of adsorbate−adsorbate interactions across the dimer pairs with different adsorbate configurations. The two surface models are presented in Figure 1.

All calculations were performed with the GAUSSIAN 94 package.[18] Analytical gradients and the hybrid density functional method including Becke's 3-parameter nonlocal-exchange functional[19] with the correlation functional of Lee−Yang−Parr,[20] B3LYP, were used for geometry optimizations with no constrained degrees of freedom. The basis set used in this paper is the standard all-electron split-valence basis set 6-31G(d)[21] including the polarization d-function on non-hydrogen atoms. Final energy parameters for both the Si_9H_{12} and $Si_{15}H_{16}$ cluster models include the unscaled zero-point-energy (ZPE) corrections calculated at the B3LYP/LANL2DZ level. Additional calculations have been made to further investigate the effect of ZPE corrections on the calculated energies using the 6-31G(d) basis set.

Results and Discussion

As referred to in the Introduction, the result of our previous work[13] for a single CO on Si_9H_{12} agrees well with that of Hu and co-workers.[11] Table 1 compares the structures, energetics, and vibrational frequencies computed with different DFT methods. In terms of bond lengths, R(C−O) is almost invariant with the level of theory while the dimer bond length $R(Si_d-Si_d)$ differs by at most 0.03 Å, from the value calculated by Hu.[11] As for the dissociation energy, our result for the OC-normal (10.6 kcal/mol) structure is in agreement with the calculated and experimental values reported by them of 14.5 and 11.5 kcal/mol, respectively. For the OC-bridge structure, we obtained a value of 2.4 kcal/mol by B3LYP/6-31G(d) and 8.4 kcal/mol by B3P86/6-31G(d, p). The latter agrees closely with that of Hu et al.,[11] 8.3 kcal/mol. The new value suggests that for OC-bridge, the extra polarization on the basis set, in addition to the electronic correlation using Perdew and Zunger[22] parametrization, increased the dissociation energy from 2.4 to 8.4 kcal/mol. The rest of the parameters for both OC-normal and OC-bridge including the C−O stretching vibrational frequency remain in good agreement with the results of Hu and co-workers.[11] The significance of this change in the OC-bridge dissociation energy will not be discussed here but will be presented in another paper in conjunction with the kinetic modeling of the adsorption and desorption of CO on the Si(100)-2×1 surface.[23]

TABLE 1: Optimized Geometries (angstroms), Binding Energies (kcal/mol), and Vibrational Frequencies (cm^{-1}) from DFT Calculations on the CO/Si_9H_{12} Cluster

	OC-normal			OC-bridge		
parameters	B3LYP/6-31G(d)	B3P86/6-31G(d, p)	ref 11	B3LYP/6-31G(d)	B3P86/6-31G(d, p)	ref 11
R(C−O)	1.144	1.142	1.144	1.194	1.192	1.191
R(Si_d−C)	1.884	1.875		1.974	1.962	1.965
R(Si_d−Si_d)	2.427	2.390	2.394	2.422	2.399	2.401
ν_{SiC-O}	2135	2151	2186	1810	1832	1831
ν_{Si-CO}	469	486		551	562	
D_e	10.6	14.2	14.5	2.4	8.4	8.3

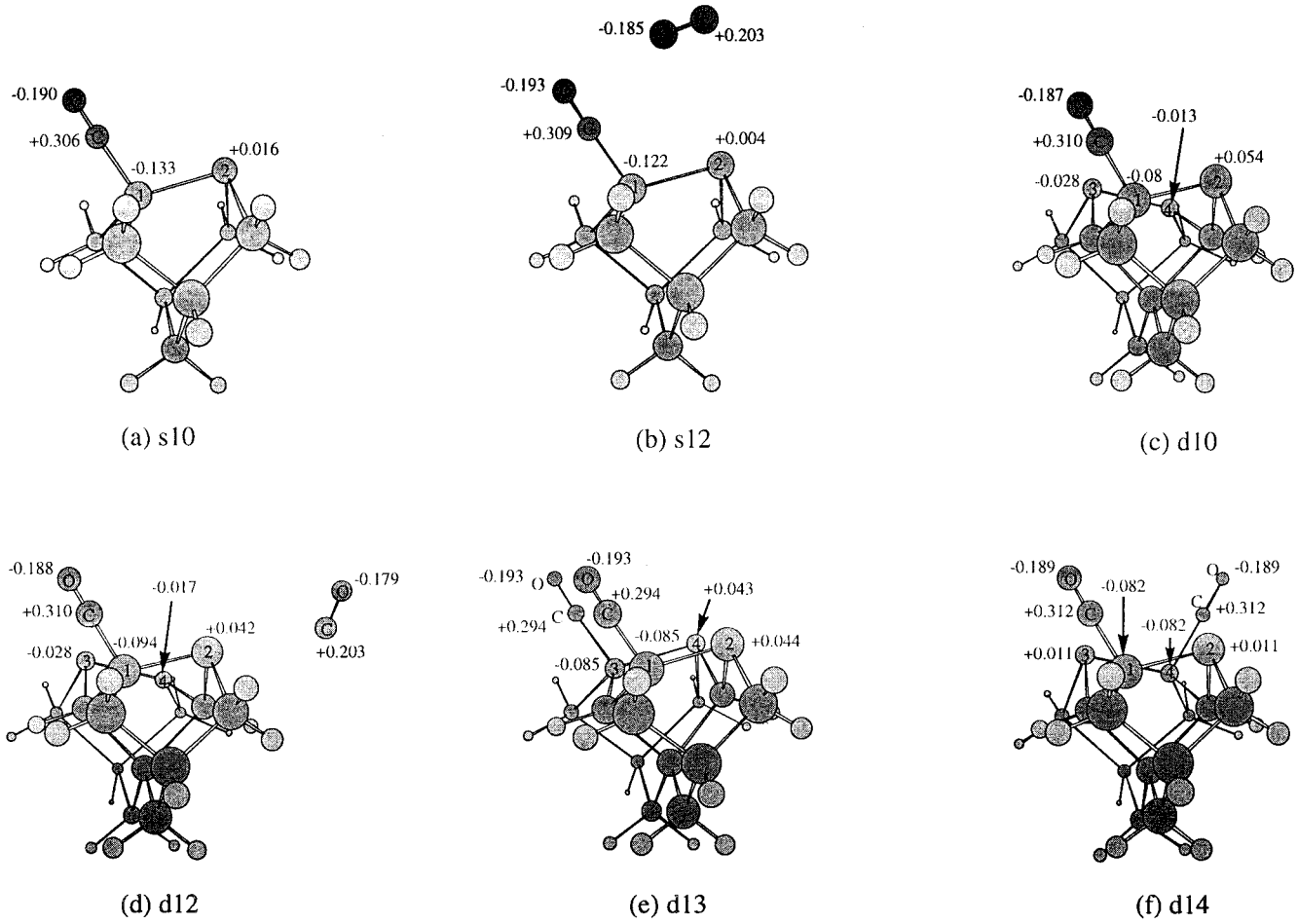

Figure 2. Optimized OC-normal geometries of the single- and double-dimer clusters including the Mulliken charges. (a) 1OC-normal.s10, (b) 2OC-normal.s12, (c) 1OC-normal.d10, (d) 2OC-normal.d12, (e) 2OC-normal.d13, and (f) 2OC-normal.d14.

To understand the CO−CO adsorbate interaction on the silicon surface, we compare the geometries as well as the energetics of the CO/Si(100)-2×1 surface using the Si_9H_{12} single- and the $Si_{15}H_{16}$ double-dimer cluster models. We perform a complete geometry optimization of the OC-normal configuration on the single-dimer model involving one and two CO molecules. We examine the adsorbate geometry and energetics and compare those with the double-dimer cluster model. In the double-dimer system, we study the four different possible adsorption combinations of the OC-normal configuration involving one and two CO molecules. Furthermore, we also investigated all the possible OC-bridge configurations for both the single- and double-dimer models with one and two CO molecules.

OC-Normal Configuration: CO Molecule Coordinating to One of the Surface Si Atoms via its C End. Figure 2 shows the different OC-normal adsorption combinations on the Si surface using the single- and double-dimer models, while Table 2 lists their optimized geometrical parameters. Adsorption of either one or two CO molecules on both the Si single- and double-dimer models elongates the Si dimer bond length by 0.2 Å, while the CO maintains its triple bond character.

As shown in Figure 2b, a second CO molecule introduced onto the single-dimer cluster is physisorbed on the Si surface dimer; the system is denoted as 2OC-normal.s12. The presence of the first CO molecule on the surface dimer prevents the second CO molecule from adsorbing chemically onto the surface dimer. This can be understood by the Mulliken charges on the surface dimer (see Figure 2). The dipole moment of the adsorbed CO induces the unoccupied Si atom to be electron deficient and also buckles the dimer. Hence, the ability of the surface to accept an additional molecule is greatly reduced. The fact that the second CO lies nearly parallel to the dimer bond may also suggest a repulsive interaction between adsorbates. In an effort to further clarify this adsorbate−surface−adsorbate interaction, we have used the optimized geometry of 1OC-normal.s10 and

TABLE 2: Optimized Geometries of the OC-Normal Configuration at the B3LYP/6-31G(d) Level Using Single and Double Dimer Models

bond length (Å)	bare Si_9H_{12} cluster	bare $Si_{15}H_{16}$ cluster	adsorbate configuration					
			1OC-normal.s10	2OC-normal.s12	1OC-normal.d10	2OC-normal.d12	2OC-normal.d13	2OC-normal.d14
1O−1C			1.144	1.143	1.143	1.143	1.144	1.143
1C−$1Si_d$			1.884	1.886	1.885	1.884	1.889	1.885
$1Si_d$−$1Si_d$	2.221	2.218	2.427	2.427	2.426	2.429	2.412	2.434
$1Si_d$−$1Si_{sub}$	2.346	2.346	2.384	2.399	2.400	2.400	2.400	2.398
2O−2C				1.139		1.138	1.144	1.143
2C−$2Si_d$				(4.452)		(3.493)	1.890	1.885
$2Si_d$−$2Si_d$		2.218			2.272	2.271	2.412	2.434
$2Si_d$−$2Si_{sub}$		2.346			2.360	2.360	2.4	2.398
$1Si_d$−$2Si_d$		4.039			3.988	3.988	3.918	3.912

TABLE 3: 2CO Adsorption on Si(100) Using Si_9H_{12} Single-Dimer and $Si_{15}H_{16}$ Double-Dimer Cluster Models with the B3LYP Method[a]

configuration	total energy (au)	D_e[b] (kcal/mol)		$D_e(2)$[c] (kcal/mol)	
		LANL2DZ	6-31G(d)	LANL2DZ	6-31G(d)
1OC-normal.s10	−2725.994 819	10.9	10.6		
2OC-normal.s12	−2839.306 272	11.7	11.7	0.8	1.0
1OC-normal.d10	−4465.393 905	17.2	16.9		
2OC-normal.d12	−4578.704 896	17.7	17.6	0.5	0.6
2OC-normal.d13	−4578.709 696	20.0	19.6	2.9	2.6
2OC-normal.d14	−4578.728 032	31.1	30.7	13.9	13.8
1OC-bridge.s12	−2725.981 871	2.2	2.4		
1OC-bridge.d12	−4465.374 955	4.8	5.0		
2OC-bridge.d12	−4578.689 582	6.2	6.8	1.4	1.7
free CO	−113.309 454				
bare Si_9H_{12} cluster	−2612.665 914				
bare $Si_{15}H_{16}$ cluster	−4352.054 911				

[a] Zero-point energy corrections have been made with the frequencies computed with LANL2DZ and 6-31G(d) basis sets. [b] Total dissociation energy where $D_e = E_{CO} + E_{Si(100)} - E_{CO/Si(100)}$ for 1CO molecule and $D_e = E_{2CO} + E_{Si(100)} - E_{2CO/Si(100)}$ for 2CO molecules. [c] Dissociation energy of the second CO molecule: $D_e(2) = E_{CO} + E_{CO/Si(100)} - E_{2CO/Si(100)}$.

coordinated a second CO molecule, through its O-end, to the buckled-up surface Si atom. We then optimized this new system to converge to its equilibrium state. The resulting configuration is the same as 2OC-normal.s12, in which the second CO is again physisorbed on the Si surface. The physisorption of the second CO molecule, therefore, is not only a function of the electrostatic interaction between the CO molecules but also a function of the induced surface charge on the dimer due to the chemisorption of the first CO molecule. Because the second CO molecule is physisorbed on the surface, the CO bond length of 1.139 Å is expected to be essentially the same as that of a free CO molecule (1.138 Å). The dissociation energy of the second CO molecule is calculated to be 1.0 kcal/mol. The energetics for 2CO adsorption on Si(100)-2×1 are summarized in Table 3. The total dissociation energies of the one-adsorbate (1OC-normal.s10) and the two-adsorbate (2OC-normal.s12) configurations using the single-dimer model have a difference of 1.1 kcal/mol at the B3LYP/6-31G(d) level of theory. This small difference corresponds to the dissociation energy of the second physisorbed CO molecule on the surface dimer.

In an effort to investigate the effect of ZPE corrections on the final energy parameters calculated with different basis sets, we have performed additional and even more expensive frequency calculations at the B3LYP/6-31G(d) level. We utilized the optimized geometries of the different adsorbate configurations at the same level of theory and calculated their vibrational frequencies for the respective ZPE corrections. Table 3 compares the B3LYP/LANL2DZ- and B3LYP/6-31G(d)-ZPE corrected dissociation energies. The results clearly indicate that the difference in the ZPE corrections between LANL2DZ and 6-31G(d) is small and has a negligible effect on the predicted desorption energies.

The double-dimer adsorbate configuration is also considered by interacting one and two CO molecules with the surface model. From Table 2 and Figure 2, the geometry of the second CO molecule adsorbed on the same surface dimer, i.e., 2OC-normal.d12, is essentially the same as that from that of the single-dimer cluster, 2OC-normal.s12. The second CO is physisorbed along the same surface dimer where the first CO is adsorbed, rendering the second surface dimer geometry almost unchanged. Moreover, as seen in Table 3, the 2OC-normal.d12 is more stable than 1OC-normal.d10 by 0.7 kcal/mol which reflects the weak binding of the second physisorbed CO molecule. At this point, it is important to compare the energies of the single-dimer clusters with the double-dimer clusters. In both 1CO and 2CO cases, comparing 1OC-normal.s10 with 1OC-normal.d10 and 2OC-normal.s12 with 2OC-normal.d12, a difference of ∼6 kcal/mol is observed in their total dissociation energies with the double-dimer clusters more energetically favorable. This difference could be attributed to the cluster size and/or surface effect of the second Si dimer in which the presence of the additional surface Si dimer lowers the total energy of the system.

Adsorption of the second CO on the second surface Si dimer is reflected in the structural changes of the cluster. As seen in Table 2, the Si dimer bond lengths for 2OC-normal.d13 and 2OC-normal.d14 become elongated by about 0.2 Å with a small relaxation of the Si_d−Si_{sub} bond distances. The second CO is chemisorbed onto the second Si dimer while maintaining its triple bond character. Furthermore, a closer look at the results in Table 3 indicates that there is an energetic preference for the 2OC-normal.d14 over the 2OC-normal.d12 and 2OC-normal.d13 structures by as much as 13 and 11 kcal/mol, respectively. In addition, the dissociation energy of 1OC-normal.d10 is higher

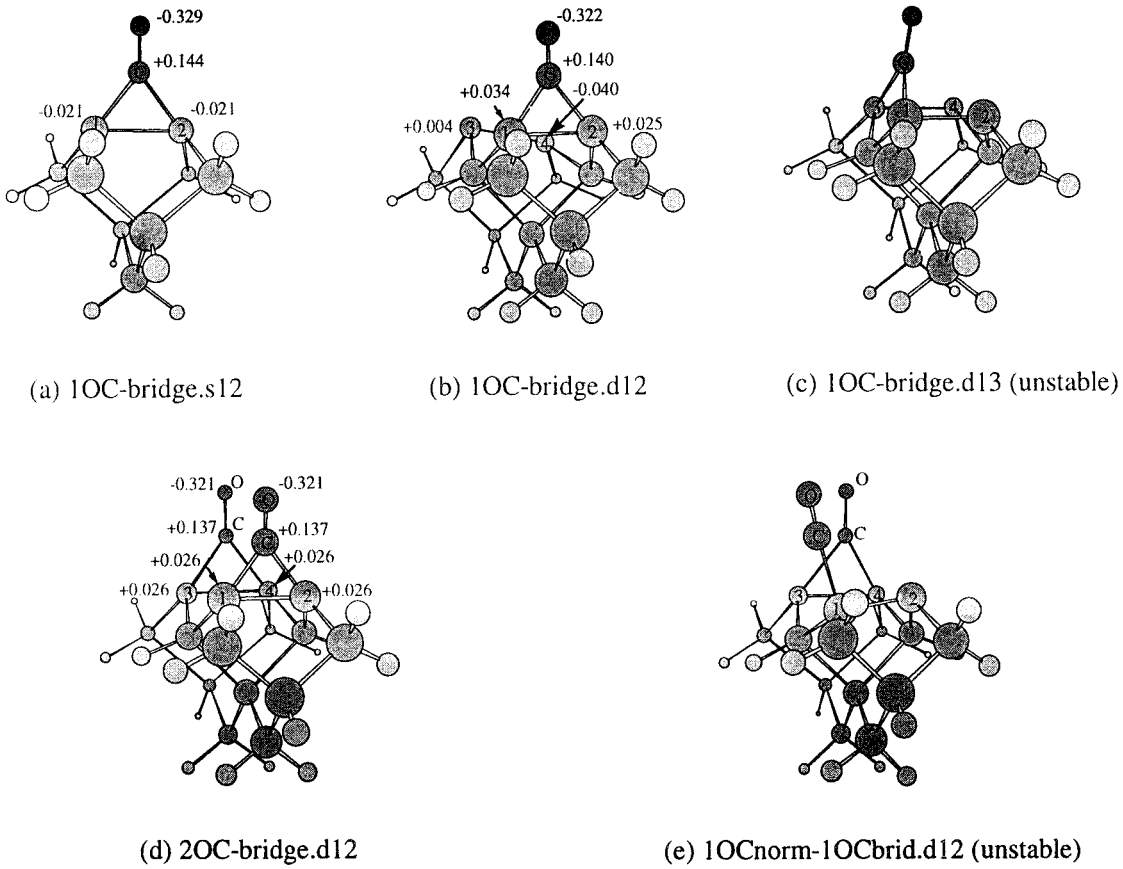

Figure 3. OC-bridge geometries using the single- and double-dimer models. All configurations are shown in their optimized geometries except (c) and (e) where they are in their initial geometries. 1OC-bridge.d13 converged to the 1OC-normal.d10 geometry while 1OCnorm-1OCbrid.d12 converged to the 2OC-normal.d14 geometry.

by 3 kcal/mol than the first CO dissociation of the 2OC-normal.d14 structure. This is indicative of the coverage dependence of the desorption energy as shown by the TPD results of Hu[11] and Breslin.[14]

There is a preference for the two CO molecules to adsorb diagonally across the two surface dimers, i.e., 2OC-normal.d14, rather than on the same end of the dimers. As indicated above, the 2OC-normal.d14 is more stable than the 2OC-normal.d13 by 11.1 kcal/mol. The Mulliken charges shown in Figures 2e and 2f suggest an electrostatic interaction between the two CO adsorbates. The diagonal configuration of the CO adsorbates in 2OC-normal.d14 minimizes the repulsion between adsorbates and enhances the Si dimer−dimer interaction due to the induced surface charge on the dimers. Although this interaction could be considered small, it is nevertheless manifested in the Si dimer−dimer separation which is shortened by 0.13 Å relative to the bare $Si_{15}H_{16}$ cluster. Furthermore, Mulliken charges for the 2OC-normal.d14 configuration are indicative of a better charge transfer from the CO molecule to the Si surface as compared with the 2OC-normal.d13 geometry. As shown in Table 2, for 2OC-normal.d14, the Si−C bond length is shorter by as much as 0.005 Å and the Si_d-Si_d bond length is more relaxed by 0.022 Å compared with the 2OC-normal.d13. With regard to the 2OC-normal.d13 structure, although the CO molecules adsorb on the same end of the surface Si dimers, a weak adsorbate−surface−adsorbate interaction may exist as the Si dimer−dimer separation is still shortened by 0.12 Å.

OC-Bridge Configuration: CO Molecule Coordinating to the Si_d-Si_d Bond via its C End. Adsorption of either one or two CO molecules on both the Si single- and double-dimer models elongates the Si dimer bond length by 0.2 Å in the OC-bridge configuration. The CO, however, no longer maintains its triple bond character; the bond is lengthened by 0.05 Å from its OC-normal configuration. Figure 3 shows the different adsorption combinations of the OC-bridge configuration and Table 4 lists their geometrical parameters.

First, we compare the structural and energy differences between the single-dimer 1OC-bridge.s12 and the double-dimer 1OC-bridge.d12. The adsorption of CO on the double-dimer model does not produce any noticeable changes in the geometry of the cluster as we compare it with the single-dimer model.[13] The CO adsorbed in a bridge configuration on the first surface Si dimer, elongating the dimer bond length by 0.2 Å as anticipated, while leaving the second surface Si dimer unchanged, almost the same dimer bond length as the bare $Si_{15}H_{16}$ cluster. As indicated by the Mulliken charges, charge transfer occurs from the Si surface dimer to the CO in both the single- and double-dimer models. Moreover, a difference of 2.6 kcal/mol is observed in their dissociation energies with the double-dimer cluster more energetically favorable.

In an effort to examine all possible configurations for the OC-bridge adsorbing onto the Si surface, we have coordinated the CO across the two surface Si dimers, i.e., 1OC-bridge.d13 (see Figure 3c). The optimized geometry and energetics of 1OC-bridge.d13 converged into the 1OC-normal.d10 configuration. This is indicative, not only of the stability of the OC-normal structure over the OC-bridge, but also of the large dimer-dimer separation which makes CO adsorption across dimers significantly less energetically favorable.

The adsorption of a second CO on the second surface Si dimer with the bridged configuration is also investigated (see Figure 3d). As seen in Table 4, the dimer bond lengths for 2OC-

TABLE 4: Optimized Geometries of the OC-Bridge Structures at the B3LYP/6-31G(d) Level for the CO−CO System Using Single- and Double-Dimer Models

			adsorbate configuration		
bond length (Å)	bare Si_9H_{12} cluster	bare $Si_{15}H_{16}$ cluster	1OC-bridge.s12	1OC-bridge.d12	2OC-bridge.d12
1O−1C			1.194	1.191	1.192
1C−$1Si_d$			1.974	1.983	1.976
$1Si_d$−$1Si_d$	2.221	2.218	2.422	2.404	2.414
$1Si_d$−$1Si_{sub}$	2.346	2.346	2.358	2.360	2.359
2O−2C					1.192
2C−$2Si_d$					1.975
$2Si_d$−$2Si_d$		2.218		2.249	2.412
$2Si_d$−$2Si_{sub}$		2.346		2.354	2.359
$1Si_d$−$2Si_d$		4.039		4.022	4.026

bridge.d12 become elongated by about 0.2 Å with some relaxation of the Si_d−Si_{sub} bond distances. The Si dimer−dimer separation (4.026 Å), however, remains almost unchanged with respect to the bare $Si_{15}H_{16}$ cluster. Although the adsorption of 2CO molecules in a bridge configuration saturates the dangling bonds on the Si surface, the unchanged dimer−dimer separation is indicative of a weak surface−adsorbate and/or adsorbate−adsorbate interaction.

Finally, we have tested the inter-configuration interaction using the double-dimer model, i.e., 1OC-normal on the first Si dimer and 1OC-bridge on the second Si dimer as denoted by 1OCnorm-1OCbrid.d12 (see Figure 3e). We have utilized the optimized structure of 1OC-bridge.d12 and added a second CO molecule in a normal configuration to the second Si dimer through the buckled down surface Si atom. Optimization of the new configuration was performed without any constraints. The resulting geometry and energy values suggest that the 1OCnorm-1OCbrid.d12 converged to the 2OC-normal.d14 configuration. This is again indicative of the higher stability of the OC-normal configuration over the OC-bridge. Another implication of our result is that, at the B3LYP/6-31G(d) level using the symmetric dimer model, the OC-normal and OC-bridge geometries could not coexist on adjacent dimers. We know from the structure of 1OC-normal.d10, as CO adsorbs onto one of the dimers, both surface dimers buckle up in opposite directions leading to electron-deficient surface Si atoms (see Figure 2c). For the OC-bridge configuration, e.g., 1OC-bridge.d12, the Si dimer with the CO coordinated in a bridge configuration remains unbuckled, whereas the unoccupied Si dimer buckles up. When a second CO molecule is introduced to the second surface Si dimer, the buckled up Si dimer atom becomes more electron-deficient due to the dipole orientation of the CO molecule. An induced surface charge due to the adsorption of the second CO molecule then shifts the electrons in the first Si dimer (with OC-bridge) from one end of the dimer to the other. This induced shift of the surface charge weakens one of the two Si−C bonds on the OC-bridge, and hence, favoring a second OC-normal configuration on the second surface Si dimer and transforming 1OCnorm-1OCbrid.d12 into 2OC-normal.d14.

Comparison with the Results of Hu et al.[11] We have compared our results with those of Hu and co-workers[11] for different surface structures as shown in Table 5. While we have performed full quantum calculations on the CO/$Si_{15}H_{16}$ dimer, Hu[11] used periodic lattice sums to estimate the effect of the periodic array of other CO on the total energy of the system. The result of our 1CO/Si_9H_{12} dimer calculation for OC-normal and OC-bridge is in better agreement with their p(2×1) phase than with their single site Si_9H_{12} calculations. Also, it is interesting to note that both Hu's[11] and our results predict the same geometry to be the most stable when all CO are in the OC-normal configuration. The estimates of Hu[11] lead to both sites having the CO in the OC-normal state on opposite Si sites,

TABLE 5: Comparison of Calculated Binding Energies (kcal/mol) for Various Surface Structures of CO on Si(100)

structure	OC-normal	OC-bridge	OC-normal/bridge combo
ref 11			
single site[a]	14.5	8.3	11.5[c]
p(2×1)[b]	12.0	3.9	
p(2×2)[b]	12.4		12.9
this work			
single site[a]	10.6	2.4	6.5[c]
2OC-normal.d14[d]	13.8[15.4]		
2OC-bridge.d12[d]		1.7[3.4]	

[a] Single-site energies are from the Si_9H_{12} dimer cluster calculations. [b] One CO per Si−Si dimer. [c] Averaged over OC-normal and OC-bridge sites. [d] Quantities in brackets are averaged values for 2OC-normal and 2OC-bridge sites, respectively.

i.e., p(2×2), just as our 2OC-normal.d14. However, they predict a configuration in which half of the CO are in OC-normal sites while the other half are in OC-bridge sites. We cannot rule out the possibility of adsorption in this configuration since we have not performed periodic lattice sum estimates. Interestingly, the probability for OC-bridge adsorption using a high-energy CO beam[11] could be accounted for with a quantum statistical model for the adsorption process. The results of our kinetic modeling will be presented in another paper as alluded to above.[23]

Conclusion

We have studied the effect of the first CO adsorbate on Si(100)-2×1 upon the adsorption of the second CO molecule using ab initio molecular orbital and hybrid density functional theory calculations. We have utilized two Si cluster models, the single-dimer Si_9H_{12} and the double-dimer $Si_{15}H_{16}$, to represent the reconstructed Si(100)-2×1 surface. From our studies, we can draw the following conclusions:

The chemisorption of a CO molecule on a Si dimer induces a change in the charge of the surface Si dimer atoms resulting to the buckling of the Si dimer. The buckled-up Si dimer atom becomes electron deficient thereby reducing the ability of the surface to accept another CO molecule on the same surface dimer. The second CO molecule is physisorbed on the surface with dissociation energy of 1.0 kcal/mol.

Adsorption of a second CO molecule on the second Si dimer is energetically preferred over coadsorption of CO on the same Si dimer. 2OC-normal.d14 is found to be the most stable configuration wherein the two adsorbed CO molecules lie diagonally across each other between the two Si dimers. The diagonal geometry minimizes the repulsion between adsorbates and enhances the Si surface dimer−dimer interaction as manifested by the shortened Si dimer−dimer separation. The dissociation energy of the chemisorbed second CO molecule is 13.8 kcal/mol (which may be compared with the experimental values of 10.7−12.7 kcal/mol).

CO adsorption across dimers is significantly less energetically favorable primarily due to the large dimer−dimer distance.

Although the adsorption of 2CO molecules in a bridge configuration saturates the dangling bonds on the Si surface, the dimer−dimer separation indicates a weak surface−adsorbate and/or adsorbate−adsorbate interaction. The Si dimer−dimer separation is found to be almost unchanged with respect to the bare $Si_{15}H_{16}$ cluster. The dissociation energy of the chemisorbed second CO molecule in a bridge configuration is 1.7 kcal/mol.

The result for the interconfiguration interaction between OC-normal and OC-bridge suggest that OC-normal is more stable than OC-bridge. Our calculations also indicate that the OC-normal could not coexist with the OC-bridge configuration on adjacent dimers due to counter-interactions between adsorbates and the induced change in the surface charge.

Acknowledgment. The calculations were performed at the Emerson Center for Scientific Computation. The authors acknowledge Dr. D. G. Musaev for helpful discussion and the research support from Emory University through the R.W. Woodruff Professorship.

References and Notes

(1) Dylla, H. F.; King, J. G.; Cardillo, M. J. *Surf. Sci.* **1978**, *74*, 141.
(2) Burton, L. C. *J. Appl. Phys.* **1972**, *43*, 232.
(3) Joyce, B. A.; Neave, J. H. *Surf. Sci.* **1973**, *34*, 401.
(4) Onsgaard, J.; Heiland, W.; Taglauer, E. *Surf. Sci.* **1980**, *99*, 112.
(5) Ibach, H.; Horn, K.; Dorn, R.; Lüth, H. *Surf. Sci.* **1973**, *38*, 433.
(6) Lee, F.; Backman, A. L.; Lin, R.; Gow, T. R.; Masel, R. I. *Surf. Sci.* **1989**, *216*, 173.
(7) Forster, A.; Lüth, H. *J. Vac. Sci. Technol. B* **1989**, *7*, 720.
(8) Chamberlain, J. P.; Clemons, J. L.; Gillis, H. P. *Desorption Kinetics of CO from Si(100)-2×1*. Presented as the 21st Annual Symposium of Applied Vacuum Science and Technology, Clearwater, FL, Feb 3−5, 1992.
(9) Bu, Y.; Lin, M. C. *Surf. Sci.* **1993**, *298*, 94.
(10) Young, R. W.; Brown, K. A.; Ho, W. *Surf. Sci.* **1995**, *336*, 85.
(11) Hu, D.; Ho, W.; Chen, X.; Wang, S.; Goddard, W. A., III *Phys. Rev. Lett.* **1997**, *78*, 1178.
(12) Imamura, Y.; Matsui, N.; Morikawa, Y.; Hada, M.; Kubo, T.; Nishijima, M.; Nakatsuji, H. *Chem. Phys. Lett.* **1998**, *287*, 131.
(13) Bacalzo, F. T.; Musaev, D. G.; Lin, M. C. *J. Phys. Chem.* **1998**, *102*, 2221.
(14) Breslin, J. Private communication.
(15) Wu, C. J.; Carter, E. A. *Chem. Phys. Lett.* **1991**, *185*, 172.
(16) Liu, Q.; Hoffmann, R. *J. Am. Chem. Soc.* **1995**, *117*, 4082.
(17) Konecný, R.; Doren, D. J. *J. Chem. Phys.* **1997**, *106*, 2426.
(18) Frisch, M. J.; Trucks, G. W.; Schlegel, H. B.; Gill, P. M. W.; Johnson, B. G.; Robb, M. A.; Cheeseman, J. R.; Keith, T.; Peterson, G. A.; Montgomery, J. A.; Raghavachari, K.; Al-Laham, M. A.; Zakrzewski, V. G.; Ortiz, J. V.; Foresman, J. B.; Peng, C. Y.; Ayala, P. Y.; Chen, W.; Wong, M. W.; Andres, J. L.; Replogle, E. S.; Gomperts, R.; Martin, R. L.; Fox, D. J.; Binkley, J. S.; Defrees, D. J.; Baker, J.; Stewart, J. P.; Head-Gordon, M.; Gonzalez, C.; Pople, J. A. *Gaussian 94*, Revision B.3; Gaussian, Inc.: Pittsburgh, PA, 1995.
(19) Becke, A. D. *J. Chem. Phys.* **1993**, *98*, 5648.
(20) Lee, C.; Yang, W.; Parr, R. G. *Phys. Rev.* **1989**, *B37*, 785.
(21) (a) Hariharan, P. C.; Pople, J. A. *Chem. Phys. Lett.* **1972**, *66*, 217. (b) Francl, M. M.; Pietro, W. J.; Hehre, W. J.; Binkley, J. S.; Gordon, M. S.; DeFrees, D. J.; Pople, J. A. *J. Chem. Phys.* **1982**, *77*, 3654.
(22) Perdew, J. P.; Zunger, A. *Phys. Rev.* **1981**, *B23*, 5048.
(23) Bacalzo-Gladden, F.; Chakraborty, D.; Lin, M. C. *Surf. Sci.* **1999**. Submitted for publication.